Localized Phase Contrast Imaging Measurements at Wendelstein 7-X

S.K. Hansen[1], M. Porkolab[1], J.-P. Bähner[1], A. von Stechow[2], O. Grulke[2,3], E.M. Edlund[4], and the Wendelstein 7-X Team

[1] *Plasma Science and Fusion Center, MIT, Cambridge, MA 02139, USA*

[2] *Max-Planck-Institut für Plasmaphysik, 17491 Greifswald, Germany*

[3] *Department of Physics, Technical University of Denmark, 2800 Kgs. Lyngby, Denmark*

[4] *State University of New York College at Cortland, Cortland, NY 13045, USA*

Localized phase contrast imaging (PCI) measurements at the Wendelstein 7-X (W7-X) stellarator have been carried out using the masking technique pioneered at the Heliotron E stellarator [1] and the DIII-D tokamak [2]. The masking technique relies on the fact that turbulent fluctuations in magnetically confined plasmas generally have wave vectors, **k**, which are almost perpendicular to the background magnetic field, **B** [1, 2]. When this is combined with the line-integrated nature of PCI measurements [1, 2, 3, 4, 5], which makes the observed **k** perpendicular to the line-of-sight (LoS) of the PCI laser beam, the direction of the **k** observed by PCI becomes a function of the pitch angle of **B** [1, 2, 3]. As illustrated in Fig. 1, the beam pattern in a focal plane of the plasma, caused by scattering off a fluctuation with wave vector **k**, consists of an unscattered beam spot and two scattered beam spots with the same shape as the unscattered one, but shifted by vectors $\propto \pm\mathbf{k}$ [1, 2]. It is therefore possible to obtain PCI measurements from a limited range of **B** pitch angles, corresponding to a limited part of the PCI LoS, by placing a mask in a focal of the PCI system, which cuts off the scattered beam spots for **k** outside the desired range of **B** pitch angles [1, 2].

The ability to obtain localized PCI measurements depends critically on the unscattered beam spot size in the focal plane where the localization mask is placed, as a scattered beam spot covering a half-angle of $\Delta\theta$ will contribute to the signal for **B** pitch angles within $\pm\Delta\theta$ of the one corresponding to its own **k**; this is illustrated in Fig. 1. To facilitate long-pulse operation, the portliner around the PCI laser beam at W7-X has been reduced in size, from previously having a radius of $a = 68\,\mathrm{mm}$, to $a = 42\,\mathrm{mm}$ in the most recent experimental campaign [5]. Since the new a is similar to the typical 1/e electric field radius of the Gaussian beam used for PCI at W7-X, $W = 40\,\mathrm{mm}$, it is of interest to determine the limit of the spot size in the focal plane imposed by the portliner. To do this, we note that, within a Fraunhofer diffraction framework, the beam pattern in the focal plane can be modeled by the Fourier transform of the truncated Gaussian, $\mathbf{E}_0^a = \mathbf{C}_0\,\Theta(a-r)\,\mathrm{e}^{-r^2/W^2}$, where $\mathbf{C}_0$ is the beam amplitude vector, Θ is the Heaviside function, and r is the distance from the beam axis. Defining the Fourier transform as

$\hat{\mathbf{E}}_0^a = \int_{\mathrm{all}\,\mathbf{x}_\perp} \mathbf{E}_0^a \mathrm{e}^{-\mathrm{i}\mathbf{k}'\cdot\mathbf{x}_\perp} \mathrm{d}\mathbf{x}_\perp$, with $\mathbf{x}_\perp$ being the coordinate perpendicular to the beam axis and $\mathbf{k}'$ being the corresponding focal plane wave vector, while noting that the intensity is $\propto |\hat{\mathbf{E}}_0^a|^2$, we find

$$|\hat{\mathbf{E}}_0^a|^2(k') = 4\pi^2 C_0^2 \left[\int_0^a r J_0(k'r)\,\mathrm{e}^{-r^2/W^2}\mathrm{d}r \right]^2, \tag{1}$$

where $J_0(k'r) = [1/(2\pi)] \int_0^{2\pi} \mathrm{e}^{-\mathrm{i}k'r\cos(\theta)}\mathrm{d}\theta$ is a Bessel function of the first kind of order zero and $k' = |\mathbf{k}'|$, $C_0 = |\mathbf{C}_0|$. When $a \to \infty$, $|\hat{\mathbf{E}}_0^a|^2(k') \to \pi^2 C_0^2 W^4 \mathrm{e}^{-k'^2 W^2/2}$, showing that the size of the non-truncated Gaussian beam spot is $\propto 1/W$. To compare the spot size with the portliner present to the Gaussian case, we fit Eq. (1) by a Gaussian function

$$|\hat{\mathbf{E}}_{\mathrm{fit}}|^2(k') = |\hat{\mathbf{E}}_{\mathrm{fit}}|^2(0)\,\mathrm{e}^{-k'^2 W_{\mathrm{eff}}^2/2}; \tag{2}$$

we also note that the 1/e beam spot radius of Eq. (2) in $\mathbf{k}'$ space is $\sqrt{2}/W_{\mathrm{eff}}$ and use this as a measure of the beam spot size in Fig. 1. Optimally, we would perform a least square fit of Eq. (2) to Eq. (1), while enforcing conservation of the power transported by the beam, i.e., $\int_{\mathrm{all}\,\mathbf{k}'} |\hat{\mathbf{E}}_0^a|^2\,\mathrm{d}\mathbf{k}' = \int_{\mathrm{all}\,\mathbf{k}'} |\hat{\mathbf{E}}_{\mathrm{fit}}|^2\,\mathrm{d}\mathbf{k}'$. Such a fit does, however, not admit a general closed form of W_{eff} and we shall therefore instead fit Eq. (1) by matching its Maclaurin series to that of Eq. (2) up to second order, which yields a simple analytical expression for W_{eff}. This method will match the least square fit in the limit of $W/a \to 0$, as both Eqs. (1) and (2) are Gaussian functions in that case. Even in the case of $W/a \to \infty$, the W_{eff} obtained by matching the Maclaurin series of Eqs. (1) and (2) up to second order only deviates from the least square fit conserving the beam power by 2.2 % [6]. Matching the zeroth order terms of the Maclaurin series yields the fit amplitude,

$$|\hat{\mathbf{E}}_{\mathrm{fit}}|^2(0) = |\hat{\mathbf{E}}_0^a|^2(0) = 4\pi^2 C_0^2 \left[\int_0^a r\,\mathrm{e}^{-r^2/W^2}\mathrm{d}r \right]^2 = \pi^2 C_0^2 W^4 (1 - \mathrm{e}^{-a^2/W^2})^2. \tag{3}$$

The first order term of the series is obtained by differentiating Eq. (1) with respect to k',

$$\frac{\partial |\hat{\mathbf{E}}_a|^2(k')}{\partial k'} = -8\pi^2 C_0^2 \left[\int_0^a r J_0(k'r)\,\mathrm{e}^{-r^2/W^2}\mathrm{d}r \right] \left[\int_0^a r^2 J_1(k'r)\,\mathrm{e}^{-r^2/W^2}\mathrm{d}r \right], \tag{4}$$

where J_1 is a Bessel function of the first kind of order one. Since $J_1(0) = 0$, it is clear that $\partial |\hat{\mathbf{E}}_0^a|^2(k')/\partial k|_{k'=0} = 0$. Differentiating Eq. (2), $\partial |\hat{\mathbf{E}}_{\mathrm{fit}}|^2(k')/\partial k' = -k' W_{\mathrm{eff}}^2 |\hat{\mathbf{E}}_{\mathrm{fit}}|^2(0)\,\mathrm{e}^{-k^2 W_{\mathrm{eff}}^2/2}$, so $\partial |\hat{\mathbf{E}}_{\mathrm{fit}}|^2(k')/\partial k'|_{k'=0} = 0$, meaning that the first order terms of the Maclaurin series will match regardless of the fit parameters, as both Eqs. (1) and (2) have stationary points at $k' = 0$. To obtain the second order term of the series, we differentiate Eq. (4) with respect to k',

$$\frac{\partial^2 |\hat{\mathbf{E}}_a|^2(k')}{\partial k'^2} = 8\pi^2 C_0^2 \left(\left[\int_0^a r^2 J_1(k'r)\,\mathrm{e}^{-r^2/W^2}\mathrm{d}r \right]^2 - \left[\int_0^a r J_0(k'r)\,\mathrm{e}^{-r^2/W^2}\mathrm{d}r \right] \times \left\{ \int_0^a r^3 \left[J_0(k'r) - \frac{J_1(k'r)}{k'r} \right] \mathrm{e}^{-r^2/W^2}\mathrm{d}r \right\} \right). \tag{5}$$

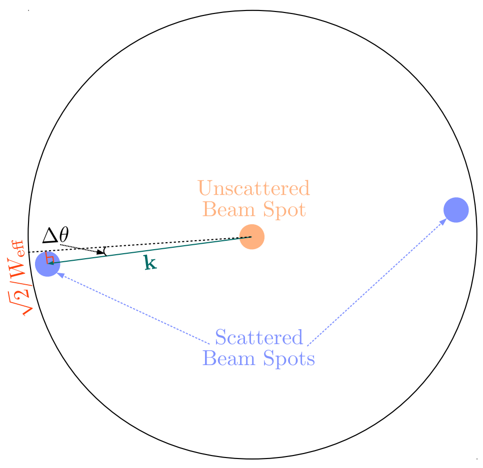

Figure 1: Beam pattern due to scattering off fluctuation with wave vector $\mathbf{k}$ in a focal plane. The scattered beam spots have the same shape as the unscattered one and their separations from it are $\propto \pm\mathbf{k}$.

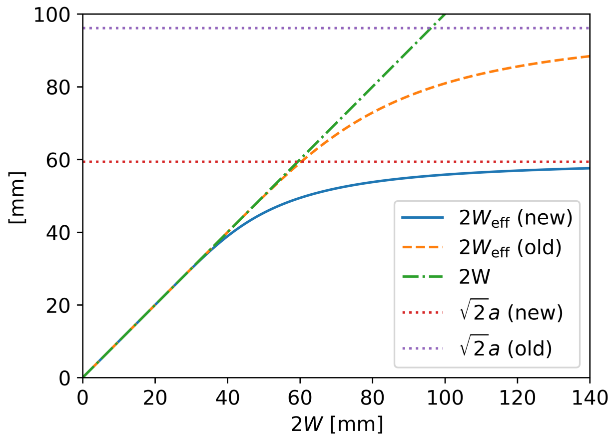

Figure 2: $2W_\mathrm{eff}$ from Eq. (7) for the new (solid line) and old (dashed line) a at W7-X, along with $2W$ (dashed-dotted line) and the new/old $\sqrt{2}a$ (dotted lines), versus $2W$. For $2W < a$, $2W_\mathrm{eff} \approx 2W$, while $2W_\mathrm{eff} \to \sqrt{2}a$ for $2W > 3a$.

Next, we evaluate Eq. (5) for $k' \to 0$, recalling that $J_1(k'r)/(k'r) \to 1/2$ when $k'r \to 0$,

$$\begin{aligned}\left.\frac{\partial^2 |\hat{\mathbf{E}}_a|^2(k')}{\partial k'^2}\right|_{k'=0} &= -4\pi^2 C_0^2 \left(\int_0^a r\,\mathrm{e}^{-r^2/W^2}\mathrm{d}r\right)\left(\int_0^a r^3\,\mathrm{e}^{-r^2/W^2}\mathrm{d}r\right) \\ &= -\pi^2 C_0^2 W^6 (1-\mathrm{e}^{-a^2/W^2})[1-(1+a^2/W^2)\,\mathrm{e}^{-a^2/W^2}].\end{aligned} \tag{6}$$

We further note that $\partial^2 |\hat{\mathbf{E}}_\mathrm{fit}|^2(k')/\partial k'^2 = (k^2 W_\mathrm{eff}^2 - 1) W_\mathrm{eff}^2 |\hat{\mathbf{E}}_\mathrm{fit}|^2(0)\,\mathrm{e}^{-k^2 W_\mathrm{eff}^2/2}$. Combining this with Eq. (3) yields $\partial^2 |\hat{\mathbf{E}}_\mathrm{fit}|^2(k')/\partial k'^2|_{k'=0} = -\pi^2 C_0^2 W^4 W_\mathrm{eff}^2 (1-\mathrm{e}^{-a^2/W^2})^2$, which finally allows us to compute W_eff by setting $\partial^2 |\hat{\mathbf{E}}_\mathrm{fit}|^2(k')/\partial k'^2|_{k'=0} = \partial^2 |\hat{\mathbf{E}}_0^a|^2(k')/\partial k'^2|_{k'=0}$,

$$W_\mathrm{eff} = W\sqrt{1 - \frac{a^2/W^2}{\mathrm{e}^{a^2/W^2} - 1}}. \tag{7}$$

For $a^2/W^2 \to \infty$, $W_\mathrm{eff} \to W$, as expected. When $a^2/W^2 \to 0$, $W_\mathrm{eff} \to a/\sqrt{2}$, in agreement with the corresponding estimate of [6]. At W7-X, $a/\sqrt{2} = 29.7\,\mathrm{mm}$, while the least square fit W_eff conserving the beam power is $0.723a = 30.4\,\mathrm{mm}$ [6], illustrating the closeness of the two fits. Figure 2 shows $2W_\mathrm{eff}$ for the old and new a at W7-X, along with $2W$ and $\sqrt{2}a$ for the old/new a, versus $2W$ up to a value of 140 mm, which is the maximum beam size allowed by the W7-X PCI system [3]. From Fig. 2, we conclude that $2W_\mathrm{eff} \approx 2W$ for $2W < a$, while $2W_\mathrm{eff}$ increases significantly slower than $2W$ for $2W_\mathrm{eff} > a$, and approaches the asymptotic limit of $\sqrt{2}a$ for $2W > 3a$. Although $2W > a$ for the typical PCI laser beam size at W7-X ($2W = 80\,\mathrm{mm}$) with both the new and old a, we note that the reduction of $2W_\mathrm{eff}$ relative to $2W$ is more significant for the new a ($2W_{\text{eff}} = 53.8\,\text{mm}$) than for the old a ($2W_{\text{eff}} = 72.9\,\text{mm}$), as expected. The above results make it possible to determine a lower limit of the **B** pitch angle which can be resolved by cutting off part of the beam in the focal plane. Using the geometry of Fig. 1, with the assumption of small $\Delta\theta$ and the fact that $W_{\text{eff}} < 0.723a$, we find

$$\Delta\theta \approx \frac{\sqrt{2}}{kW_{\text{eff}}} > \frac{1.956}{ka}. \tag{8}$$

Equation (8) illustrates that it is generally easier to localize modes with larger k, as their scattered beam spots cover a smaller angle, in agreement with [1, 2] and Fig. 1. The experimental $\Delta\theta$ limit is expected to be somewhat larger than that of Eq. (8) due to diffraction effects beyond the Fraunhofer model [2], but Eq. (8) still serves as an ultimate lower bound. For the new typical effective beam radius at W7-X ($W_{\text{eff}} = 26.9\,\text{mm}$) and ion temperature gradient (ITG) driven modes around $k \approx 6\,\text{cm}^{-1}$, which have the largest linear growth rate for standard electron cyclotron resonance heated plasmas at W7-X [4], $2\Delta\theta \approx 10^\circ$ from Eq. (8). On the other hand, the variation of the pitch angle of **B** along the PCI LoS ranges from 15° to 20° on the outboard side of W7-X in different magnetic configurations [3]. Using these estimates, we thus see that localization of typical ITG turbulence PCI features down to half the minor radius is feasible on the outboard side of W7-X. On inboard side of W7-X, the variation of the pitch angle of **B** along the PCI LoS is approximately 5° in all magnetic configurations [3] and the ability to obtain localized PCI measurements on the inboard side is rather limited as a result. Detailed results related to the W7-X PCI localization masks will be presented in a future publication.

Acknowledgments

Support for the MIT and SUNY-Cortland participation was provided by the US Department of Energy, Grant DE-SC0014229. This work has been carried out within the framework of the EUROfusion Consortium, funded by the European Union via the Euratom Research and Training Programme (Grant Agreement No 101052200 – EUROfusion). Views and opinions expressed are however those of the author(s) only and do not necessarily reflect those of the European Union or the European Commission. Neither the European Union nor the European Commission can be held responsible for them.

References

[1] S. Kado et al., *Jpn. J. Appl. Phys.* **34**, 6492 (1995)
[2] J.R. Dorris, J.C. Rost, and M. Porkolab, *Rev. Sci. Instrum.* **80**, 023503 (2009)
[3] Z. Huang et al., *J. Instrum.* **16**, P01014 (2021)
[4] J.-P. Bähner et al., *J. Plasma Phys.* **87**, 905870314 (2021)
[5] S.K. Hansen et al., *Plasma Phys. Control. Fusion* **64**, 095011 (2022)
[6] B. Zhang, J. Zerubia, and J.-C. Olivo-Marin, *Appl. Opt.* **46**, 1819 (2007)